Paris, France - August, 2025 Paper No. HTFF 242 DOI: 10.11159/htff25.242

Assessment of Influence of Flow Regime on Heat Transfer Capacity of A Shell and Tube Heat Exchanger Using Computational Fluid Dynamics Analysis

S.A.P Ushettige¹, W.K. Wimalsiri², H.G.S. Hikkaduwa³

¹Faculty of Engineering, School of Civil and Mechanical Engineering, Curtin University, Bentley, WA 6102, Australia

20545756@student.curtin.edu.au; walallawita.w@sliit.lk

²Faculty of Engineering, Mechanical Engineering, Sri Lanka Institute of Information Technology Malabe, 10115, Sri Lanka

³Faculty of Engineering, General Sir John Kothalawala Defence University Kandawala Road, Dehiwala-Mount Lavinia, 10390, Sri Lanka hikkaduwahgs@kdu.ac.ok

Abstract – Shell and tube heat exchangers (STHX) are widely adopted in industrial thermal systems due to their reliability and performance. As such thermo-mechanical design and sizing of these devices has become a continuously expanding and existing research domain. Following technological advancements, CFD is now widely adopted for flow analysis and design. An upcoming area as of recent is the integration of tools such as non-linear least squares regression and CFD to develop correlations capable of predicting thermal performance based on the input design parameters such as *Re* and *Pr*. However, limited applications exist for STHXs. This study focuses on the development of thermal correlations in the form of $Nu = C.Re^a.Pr^b$ for a small TEMA E-type STHX. For these devices, turbulence is identified as a key parameter which affects thermal and mechanical performance and is often introduced by using metal plates known as baffles. Single segmental baffles which are widely used in industry are integrated into the design. Hence, turbulence is varied as a function of both the mass flow rate and the central spacing among the baffles. CFD Modelling in ANSYS-Fluent is conducted in the steady state for six, eight, ten and twelve baffles. Following CFD analysis the data is fit using non-linear least squares regression in MATLAB Curve-Fitter Toolbox generating four correlations with applicable operating ranges. The results of the goodness of fit were reasonable, however, high 95 % confidence interval widths were evident for certain fitted coefficients leaving further potential for improvement. The work conducted highlights that the application of CFD combined with numerical tools such as non-linear least squares regression can act as an aid in the design and optimization of heat exchangers, increasing design potential for engineers and researchers.

Keywords: CFD, Shell and tube heat exchangers, Non-linear least squares regression, Baffle spacing, Design Optimization, Heat Transfer

1. Introduction

Heat exchangers are devices which are used for the transfer of thermal energy in industrial processes with a range of applications in both the commercial and domestic sectors [1]. Among the range of types present, shell and tube heat exchangers are widely used due to mechanical reasons [2, 3]. The key reason behind its use is the ability to provide a large amount of heat transfer area for a given volume and ease of construction. Exchange of thermal energy in these devices are achieved by a combination of conduction and convection phenomena due to the flow of fluid inside the tubes and the shell [4]. This can be visualised through the schematic shown in Figure 1 (a) below.

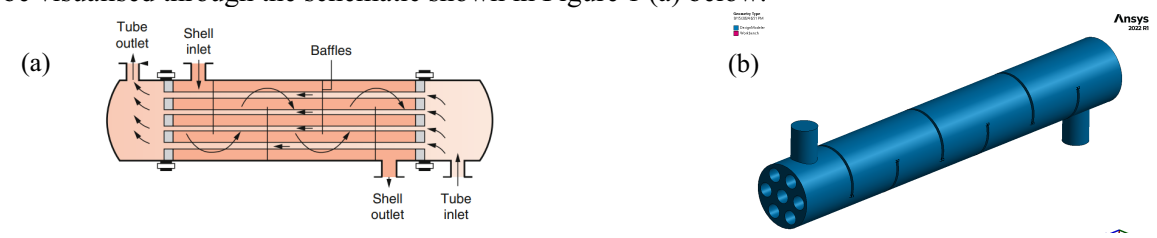


Figure 1: (a) Schematic of Single Pass TEMA E Type STHX [5](b) ANSYS Physical Model.

Given their application in several energy intensive industries, design and sizing are critical, of which pressure drop, and heat transfer analysis are the centre of the evaluations [6,7]. Traditional design methods such as those recognized and developed by leading organizations such as Tubular Exchangers Manufacturers Association (TEMA) of the USA utilized empirical correlations, these were limited by the inability to visualize the flow field in the shell volume [8]. A consequence was designers lacked the capacity to identify design weaknesses, limiting possibility for design and optimization [9]. This led to the adoption of computational fluid dynamics modelling for the assessment of thermo-mechanical performance. A range of software such as Ansys Fluent, Ansys CFX, FIDAP, CFD2000, STAR CD and PHEONICS are now employed industrially [3].

The level of turbulence has a significant impact on thermo-mechanical performance where it is commonly introduced and controlled using metal plates known as baffles. Several configurations and types exist, including single, double, and triple segmental, as well as helical, flower, rod, and overlapping baffles [10,11]. Among these, single segmental baffles are commonly used; however, they come with associated drawbacks [2,9,12,13,14,15]. "Dead zones" or areas of recirculation are produced behind baffle, this impacts heat transfer negatively as the amount of heat transfer contact area is reduced. Additionally, high values of nozzle-to-nozzle pressure drop are also present due to significant flow expansion and contraction along the path within baffle window regions.

Optimization of thermo-mechanical performance by the variation of baffle parameters such as configuration, type, central baffle spacing and baffle cut is an existing and continuously expanding research domain. Among these, central baffle spacing and baffle cut are highlighted as critical design parameters which affects the flow phenomena and performance as indicated in Figure 2(a) according to [9] and [14]. Decreasing the baffle spacing has been found to decrease the size of recirculation areas, hence, improving thermal performance [9, 14]. However, this is associated with an increase in pressure drop due to increased obstruction to the fluid flow.

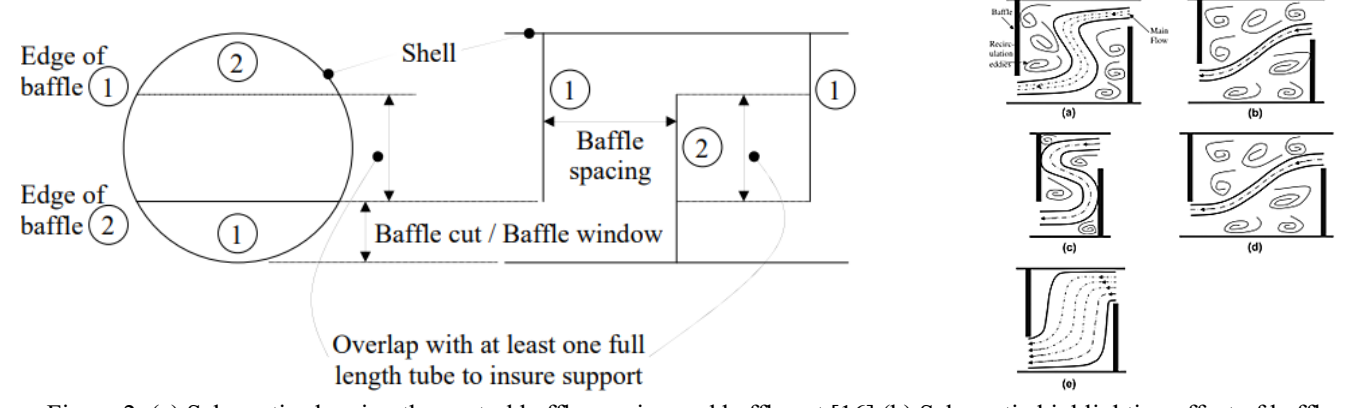


Figure 2: (a) Schematic showing the central baffle spacing and baffle cut [16] (b) Schematic highlighting effect of baffle cut and spacing on flow phenomena [9].

In the recent research work, researchers have started combining CFD with numerical methods such as non-linear least squares regression to develop correlations to aid thermal design. However, following a comprehensive survey of literature very limited applications were present for shell and tube heat exchangers. Well established examples, include the work done by [17] who evaluated the thermal performance of nano-fluid moving within a horizontal counter-flow double tube heat exchanger and study done by [18] who worked towards developing corelations which can predict the Nu for the air side of each individual row in a plate-fin and tube heat exchanger. These studies utilized non-linear least squares regression to develop correlations which can relate the Nu to the input design parameters (Pr and Re) of the flow. Additionally, building on the work done by [18] the study done by [19] highlighted that there was little to no sensitivity to different modelling schemes utilized further building the ground for their application.

This study will utilize the commercial CFD package ANSYS Fluent ® to explore the thermo-mechanical performance of a small TEMA E-TYPE single pass shell and tube heat exchanger with the working fluid considered as water. The model was selected following its adoption in a range of published literature in the existing research domain [2,9,12,13,14,15]. The

shell side is resolved considering state steady simulations, with varying inlet mass flow rates in the range of 0.5 kg/s to 2.0 kg/s in increments of 0.25 kg/s. The effect of turbulence level (*Re*) is explored by varying both the inlet mass flow rate and the central baffle spacing by simulating for six, eight, ten and twelve baffle models. Detailed flow analysis is performed by resolving the shell side velocity and pressure contours. The findings are then validated against a range of published literature.

This study is a comprehensive extension of those present in literature where the effect of Re on thermo-mechanical performance is explored in detail after which an effort is made to develop correlations in the form of $Nu = C.Re^a.Pr^b$. This is achieved by combining non-linear least squares regression in MATLAB with the CFD based results. The research work highlights the application and the ability to extend the developed workflow to aid thermal design of larger scale shell and tube heat exchangers.

2. Methodology

2.1 Physical Modelling

The models of the heat exchangers were made by ANSYS Design modeler where the volume of the baffles were neglected in the simulation. A 3D view of the six-baffle model is shown in Fig. 1 (b) above. The key dimensions of the model are shown in Table 1 below [9]. Water is selected as the shell side fluid and Aluminum is used for the surface of the tubes. The standard properties present in the ANSYS Fluent database are used. Piece-wise linear interpolation was not used given the operating temperature range was narrow. The simulations are conducted in a steady state, this follows from the assumption in similar studies [9, 12, 15].

Dimensional Parameter	Value / mm
Diameter of the shell	90
Outside diameter of the tubes	20
Number of tubes used	7 tubes
Length of the heat exchanger	600
Central baffle spacing	86

Table 1: Dimensions of the shell and tube heat exchanger [9].

2.2 Turbulence Modelling and Boundary Conditions

The turbulence in the shell side of the heat exchanger is modelled using the standard k- ε turbulence model where the model suitability is highlighted in studies done by [3],[9] and [14]. The key highlights of the model include reasonable capture of flow detail, low computational time and simple closure offered. Secondly, the inlet and outlet boundary conditions applied at the nozzles are the standard mass flow and pressure boundary conditions respectively [9, 12, 14, 15]. Following the assumption of steady state, a zero-heat flux condition and fixed thermal condition of 450 K are applied to the shell wall and tubes respectively.

2.3 Computational domain, mesh and model choices

The heat exchanger flow domain is modelled using an unstructured tetrahedral mesh with the aid of the ANSYS Meshing Tool (refer Figure 3(a)). Four grids of element numbers \sim 1.2 million, \sim 2.2 million, \sim 3.3 million and \sim 5.0 million were generated. The variation of the overall heat transfer coefficient was monitored for all grids. Considering that the difference among the 3.3 and 5.0 million grid was less than 2.0 %, the grid with 3.3 million elements was selected. The discrepancy observed is similar to that observed in studies done by [14] who worked on similar type of analysis.

Another factor which affects the thermal results is the near wall behaviour at the tube surfaces. The accurate capture of the near wall flow in the model was ensured by using prism layers near the tube surface (refer Figure 3(b)). Additionally, a scalable wall function was used to limit the $y^+ \approx 11.5$ such that the flow is compatible with the standard k- ε turbulence

model [13, 20]. This non-dimensional parameter represents the distance from the wall to the first node and is an important parameter defining near wall flow in CFD [20]. Resolution of the near wall flow exhibited variations which can be attributed to the flow expansion and contraction, where certain areas exhibited values below the cutoff y^+ . However, its overall effect on the bulk quantities analyzed were insignificant.

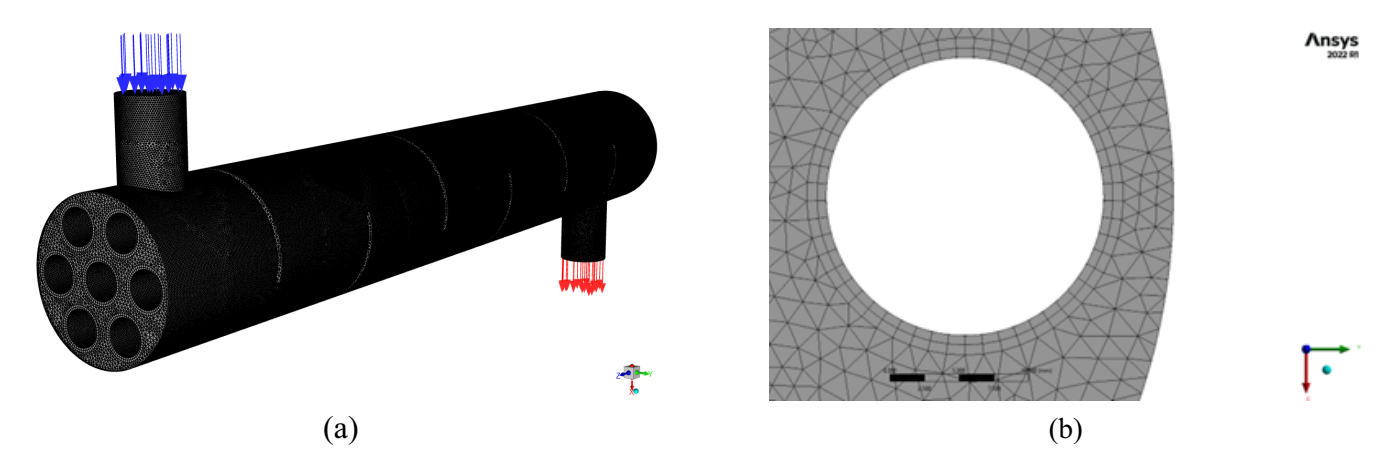


Figure 3: (a) Meshed model with boundary conditions (b) Zoomed in view of the near wall mesh.

A target residual tolerance of 10^{-3} was used for the model solution. Based on a survey of existing research this is selected based on the expected level of detail. Considering a range of studies, this appears to be a balance between accuracy and computational power.

2.4 Correlation development using Nonlinear least squares regression (NLSQR)

Non-linear least squares regression is used to develop the correlations which relate the Nu to the Pr and Re. The approach of using CFD for correlation prediction has been applied for plate fin heat exchangers as evident in studies done by [18] and [19] with minimal adoption seen for shell and tube heat exchangers. NLSQR is applied using MATLAB Curve Fitter Toolbox. Given the variation of the flow regime and thermal performance in the four models, four sets of correlations of the form Nu = C, Re^a , Pr^b are developed using the CFD results. The formulation is similar to that used in recognized thermal design methods such as the Kern's method, Bell-Delaware method and the flow-stream analysis method [21]. Equations 1-3 below, show the derivation of the Re based on the principles used in established design methods [22], similar analogies are used for estimation of the Nu and Pr.

$$D_e = \frac{4\left(\frac{P_t}{2} * 0.87 * P_t - 0.5 * \pi * \frac{d_o^2}{4}\right)}{\pi^* \frac{d_o}{2}}$$
(1)

$$A_{S} = \frac{(P_{t} - d_{o}) * D_{S} * B}{P}$$
 (2)

$$A_{s} = \frac{(P_{t} - d_{o})^{*} D_{s}^{*} B}{P_{t}}$$

$$Re = \frac{\left(\frac{\dot{m}_{s}}{A_{s}}\right)^{*} D_{e}}{\mu}$$
(2)

Results And Discussion

4:

3.1 Thermo-mechanical results for the four models

CFD results indicate that the overall heat transfer coefficient, total heat transfer rate and shell side pressure drop increase with the mass flow rate as shown in Figure 4 (a) and (b) below for the six-baffle model. The differences observed in the trend could be attributed to variations in grid resolution, type, quality, level of convergence and types of turbulence models used. The results obtained in [2] support this statement given they utilized a similar grid type and turbulence model.

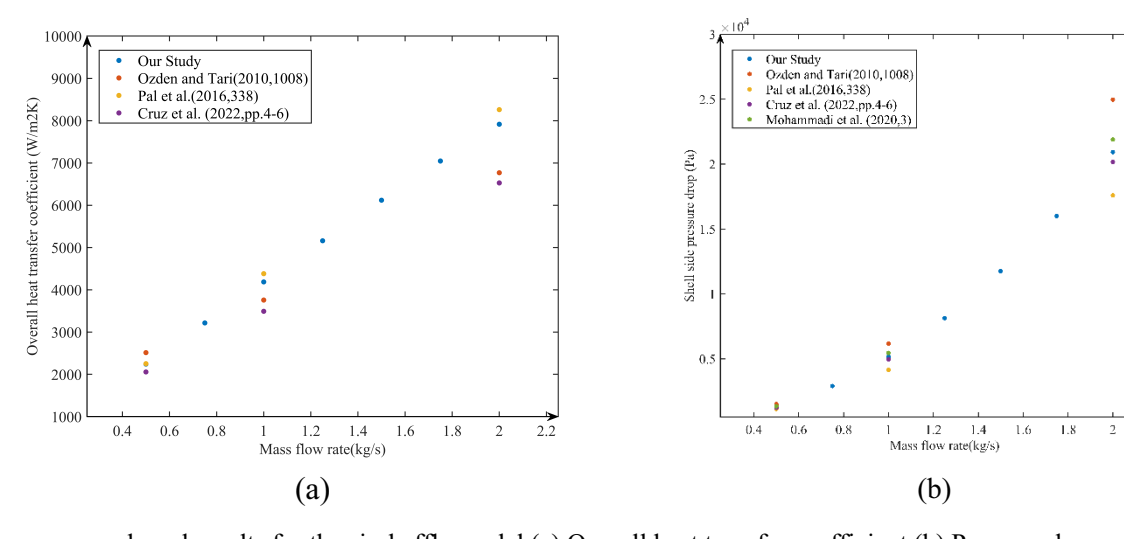


Figure CFD

based results for the six-baffle model (a) Overall heat transfer coefficient (b) Pressure drop.

Increasing the number of baffles was observed to significantly affect the thermal and mechanical performance as indicated in Table 2 below. The impact on thermal performance is positive, where the improvement can be related to the enhancement of the shell side flow phenomena or streamlines. Pressure drop is impacted adversely by requiring higher mechanical pumping power to maintain the fluid flow. Both the underlying phenomena will be analyzed in the context of the streamlines and pressure contours in the next section prior to the results of CFD based correlations.

Table 2: CFD based results for the eight, ten and twelve baffle models.

Nb	Mass flow rate	Temperature Rise Shell Side/ K	Total heat transfer / W	Heat transfer Coefficient/ W/m ² K	Shell Side Pressure/ Pa
	0.5	341.0	86108.8	2541.5	1796.0
8	1.0	339.8	163658.1	4787.7	7265.0
	2.0	337.1	311113.1	9028.6	28977.0
	0.5	334.6	93488.1	2802.6	2504.1
10	1.0	342.5	178466.0	5301.4	10112.8
	2.0	340.7	341102.01	10050.9	40372.8
	0.5	347.4	99332.4	3015.6	3303.4
12	1.0	345.3	190088.6	5717.6	13323.7
	2.0	338.4	365346.1	10900.3	53066.1

3.2 Velocity Streamline variation with baffle spacing

Velocity streamlines reveal the fluid flow and its dependence on the baffle spacing (refer Figure 5(a)-(c)). At the highest baffle spacing (six baffle), significantly large areas or recirculation are evident which are indicated by streamlines in light blue colour. Decreasing the baffle spacing is seen to improve the shell side flow phenomena, with smaller areas of recirculation and a more uniform flow path being produced eventually. This decreases the amount of tube area bypassed by the fluid flow, hence, increasing the amount of heat transfer [9,14]. At the lowest baffle spacing (ten and twelve baffles) minimal recirculation is evident, however, similar studies done by [9] state that no areas of recirculation are evident. This difference could be attributed to the differences in the modelling.

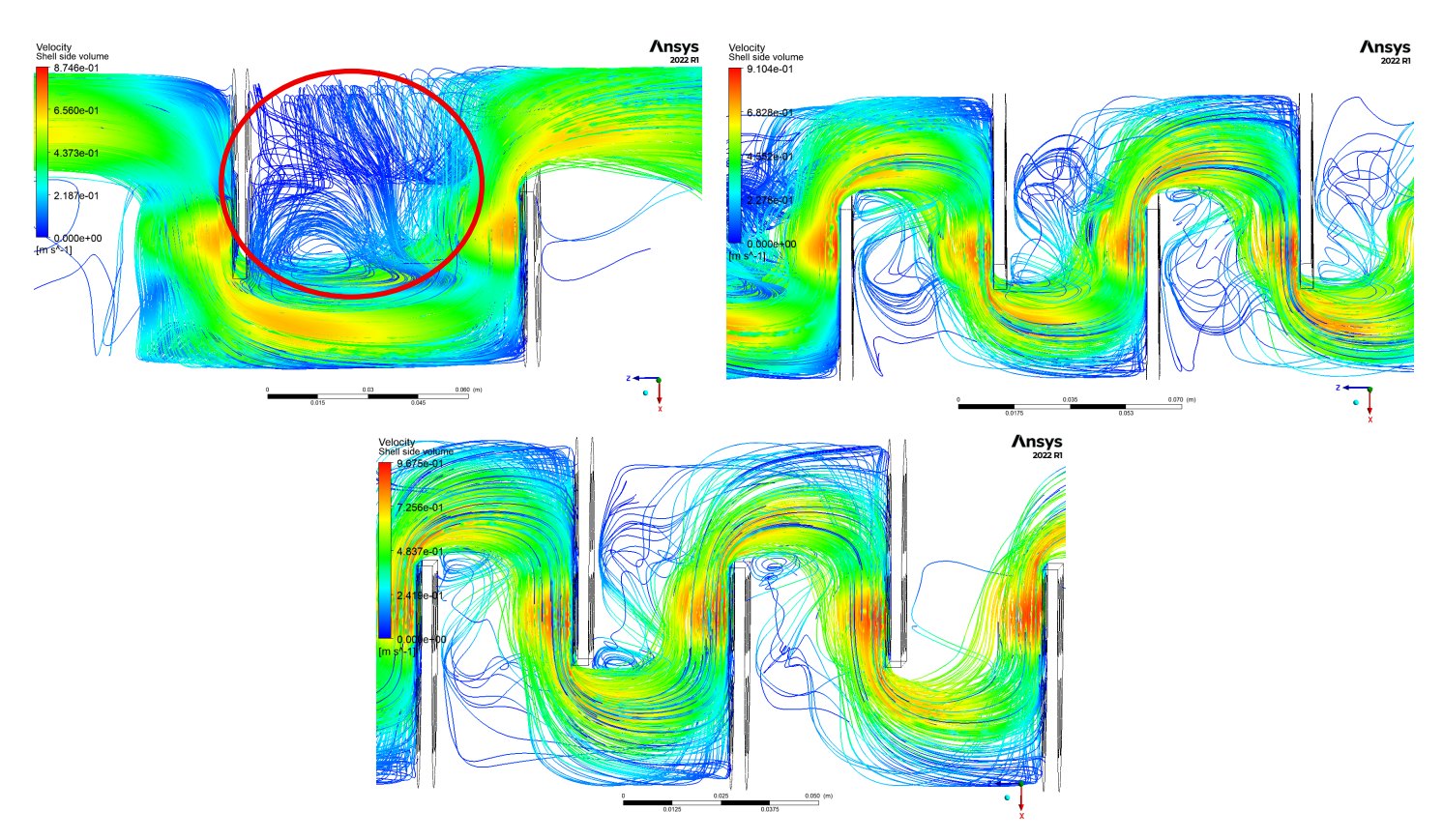


Figure 5: Velocity streamlines at 0.5 kg/s (a) 6 baffles (b) 10 baffles and (c) 12 baffles.

3.3 Pressure drop variation with length

The nozzle-to-nozzle pressure drop is observed to decrease along the length of the heat exchanger with the highest-pressure present at the inlet nozzle where the fluid impingement happens (refer Fig. 6 (a) and (b)). Similar contours are seen for both the lowest and the highest flow rates with minimal difference present. Contours reveal the presence of localized pressure at baffle windows; this is a consequence of significant flow contraction. In addition, the relatively prominent pressure gradients present at the inlet and outlet could be attributed to the impingement of fluid within the nozzle [29].

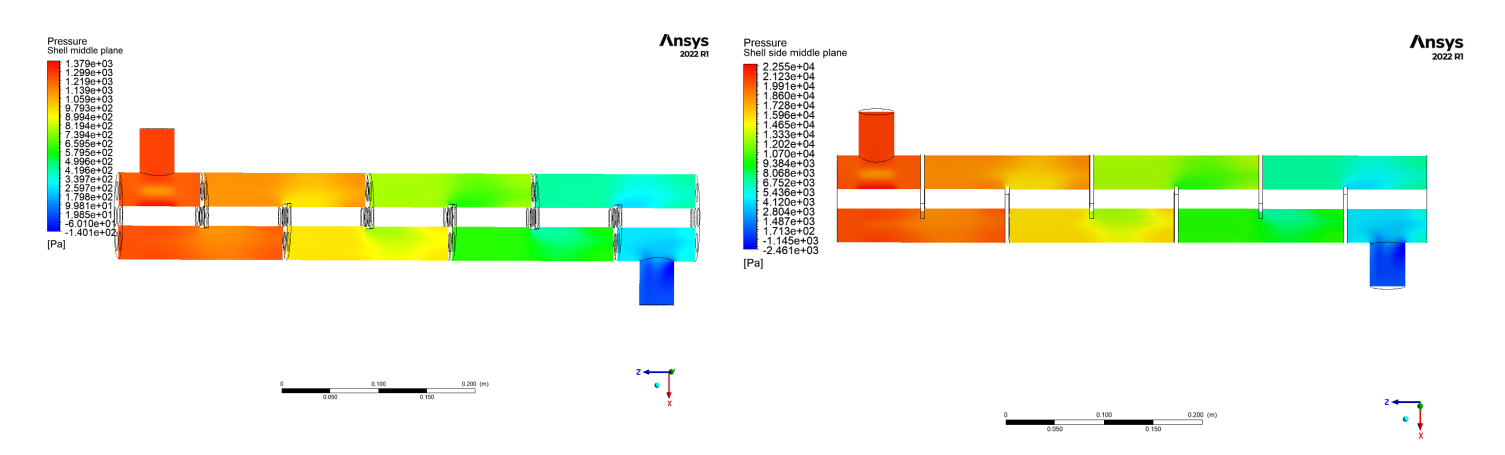


Figure 6: (a) Variation of pressure along the heat exchanger length (a) 0.5 kg/s (b) 2.0 kg/s

The contours indicate the presence of a negative back pressure at the outlet; this could be attributed to improper flow development which was identified following analysis of the flow at the plane of the outlet nozzle. A similar phenomenon was observed in studies done by [2] and [23].

3.4 CFD-Based Correlations for the four models

The non-dimensional parameters Nu, Re and Pr were determined for the four models respectively using similar analogies to that in the established Kern's and Bell-Delaware thermal design methods. Then NLSQR was used to fit the data as indicated in Figure 7(a) and (b) below.

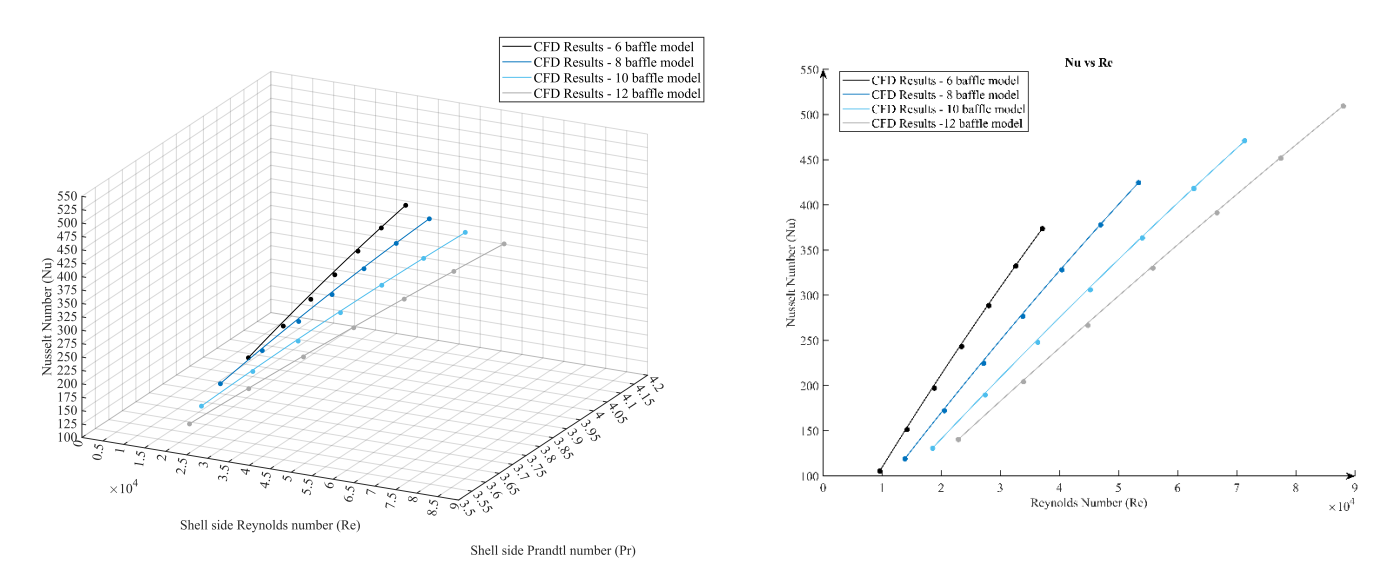


Figure 7: (a) Variation of Nu vs Re, Pr for all four models (b) Variation of Nu vs Re for all four models.

Nu is observed to significantly increase with the Re, where Re is a function of both the increasing mass flow rate and decreasing baffle spacing. The observed correlation arises from the improvement of the shell side flow phenomena as revealed earlier in the flow contours and in similar studies such as that done by [9] and [14]. In addition, the range of Pr is minimal given that the shell inlet temperature was kept constant. Slight decreases in Pr observed with increasing baffle

number could be related to the variations in thermal properties with temperature. A summary of the correlations formulated are shown in Table 3 below, with the applicable ranges of the *Re* and *Pr* for the four models.

 \boldsymbol{C} **Baffles** b Re Range Pr Range 9605.7 < *Re* < 37104 3.678 < Pr < 4.1240.9972 -2.19076 0.2312 13864 < Re < 53405 3.7981 < Pr < 3.95898 0.139 1.0065 -2.130418543 < Re < 71364 10 -1.9586 3.6554 < Pr < 3.81350.0809 1.0103 22892 < Re < 8805712 0.0319 0.9964 -1.27353.5437 < Pr < 3.6986

Table 3: Summary of the correlations developed for all four models.

Reliability and precision of the formulations can be determined using the confidence interval (CI) width of each evaluated term [24]. The traditionally used confidence level of 95 % was used, however, this can sometimes lead to the confidence level not being useful given the higher width [25]. CI widths for the model parameters are indicated in Table 4 below.

Table 4: Summary of the 95 % confidence interval widths for six, eight, ten and twelve baffle models.

Nb	6			8		
Parameter	Predicted value	Lower bound	Upper bound	Predicted value	Lower bound	Upper bound
\boldsymbol{C}	0.2312	0.014	0.4485	0.1390	0.0158	0.2623
а	0.9972	0.9758	1.0186	1.0065	0.9817	1.0312
b	-2.1907	-3.0117	-1.3696	-2.1304	-2.9624	-1.2914
Nb	10			12		
Parameter	Predicted value	Lower bound	Upper bound	Predicted value	Lower bound	Upper bound
C	0.0809	0.0263	0.1355	0.0319	0.0207	0.0431
а	1.013	0.9900	1.0307	0.9964	0.9852	1.0076
b	-1.9586	-2.6318	-1.2854	-1.2735	-1.639	-0.908

The confidence interval width is observed to decrease with the increase in number of baffles. This indicates an improvement in both the stability and the curve fit, which can be further highlighted using the goodness of fit statistics as indicated in Table 5 below.

Table 5: Summary of the SSE and RMSE for the six and twelve baffle models.

Baffles	SSE (Sum of Squares due to Error)	RMSE (Root Mean Squared Error)	
6	0.2064	0.1703	
12	0.1279	0.0654	

Goodness of fit statistics observed indicate that the random component of error present in the model is minimal, emphasizing that the model is suitable for use as a prediction tool. Figure 8 below shows the residual plot for the six and twelve baffle models. The lower magnitude of residuals presents in the twelve-baffle model highlights the improvement in the CI of the coefficients and hence the reliability of the model. Overall, the predicted correlations can be utilized with reasonable confidence for similar models given the operating range of the non-dimensional parameters are known.

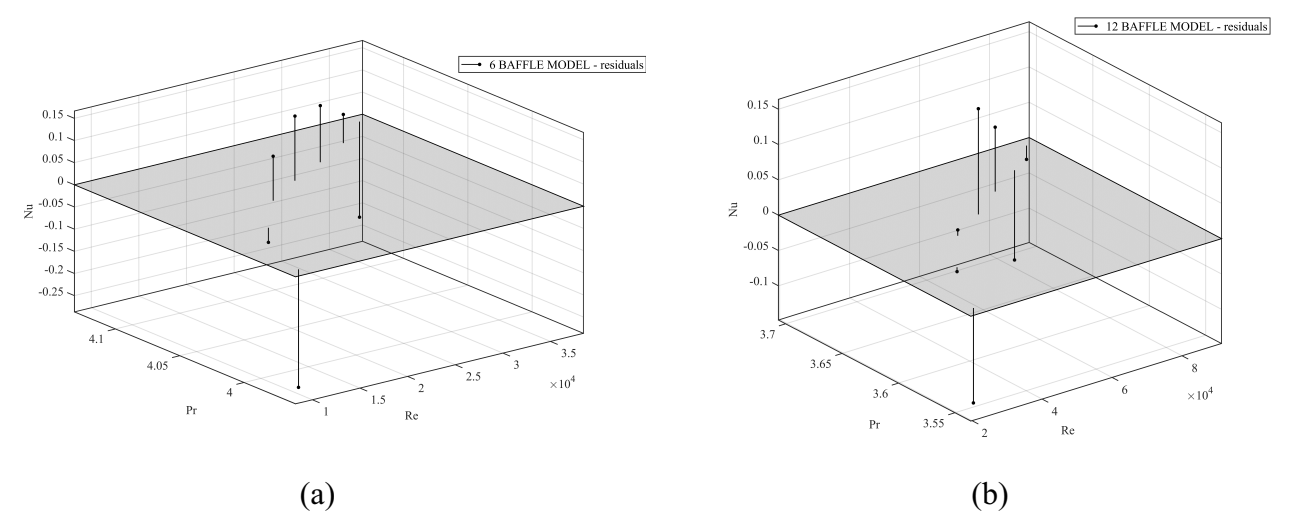


Figure 8: Residual plots for (a) six baffle model (b) twelve baffle model.

4. Conclusion

CFD based visualization of fluid flow in this study highlighted the effect of central baffle spacing on both thermal and mechanical performance of a small TEMA E-type shell and tube heat exchanger. This was successfully captured by considering four baffle spacings (six, eight, ten and twelve baffles). Visualization revealed that decreasing the baffle spacing minimizes recirculation areas and enhances thermal performance at the expense of a higher pressure drop. The developed set of CFD based correlations for the four models allows to predict the thermal performance based on the key input design parameters (*Re* and *Pr*), with a relatively high confidence. Overall, the workflow developed, and the correlations can be used for the thermal design of similar models. The research work highlights the potential of combining CFD with tools such as non-linear least squares regression to aid the process of thermal design and management by developing correlations capable of predicting thermal performance based on the design parameters. Future work can focus on improving the quality of the grid, turbulence modeling, and model convergence, resolving the flow in the tube side, consideration of a range of inlet conditions, and applying tools such as ANN (Artificial Neural Networks) and frameworks capable of making decisions to improve the accuracy of the model and the optimization process.

References

- [1] M. Mohanraj, S. Jayaraj, and C. Muraleedharan, "Applications of artificial neural networks for thermal analysis of heat exchangers A review," International Journal of Thermal Sciences, vol. 90, pp. 150–172, 2015. [Online]. Available: http://dx.doi.org/10.1016/j.ijthermalsci.2014.11.030
- [2] E. Pal, I. Kumar, J. B. Joshi, and N. K. Maheshwari, "CFD simulations of shell-side flow in a shell-and-tube type heat exchanger with and without baffles," Chemical Engineering Science, vol. 143, pp. 314–340, 2016. [Online]. Available: http://dx.doi.org/10.1016/j.ces.2016.01.011
- [3] M. M. Aslam Bhutta, N. Hayat, M. H. Bashir, A. R. Khan, K. N. Ahmad, and S. Khan, "CFD applications in various heat exchangers design: A review," Applied Thermal Engineering, vol. 32, no. 1, pp. 1–12, 2012. [Online]. Available: http://dx.doi.org/10.1016/j.applthermaleng.2011.09.001
- [4] I. A. Fetuga, O. T. Olakoyejo, S. M. Abolarin, J. K. Gbegudu, A. Onwuegbusi, and A. O. Adelaja, "Numerical analysis of thermal performance of waste heat recovery shell and tube heat exchangers on counter-flow with different tube configurations," pp. 859–875, 2023.
- [5] M. N. Özişik, Heat transfer: a basic approach. New York St Louis Paris [etc.]: McGraw-Hill, 1985.
- [6] Z. Huang, Y. Hwang, and R. Radermacher, "Review of nature-inspired heat exchanger technology," International Journal of Refrigeration, vol. 78, no. 2017, pp. 1–17, 2017. [Online]. Available: http://dx.doi.org/10.1016/j.ijrefrig.2017.03.006
- [7] B. Sundén, "Heat exchangers and heat recovery processes in gas turbine systems," Modern Gas Turbine Systems: High Efficiency, Low Emission, Fuel Flexible Power Generation, no. 2006, pp. 224–246, 2013.
 - [8] K. Thulukkanam, Heat Exchangers. Boca Raton: CRC Press, feb 2024. [Online]. Available: https://www.taylorfrancis.com/books/9781003352044
- [9] E. Ozden and I. Tari, "Shell side CFD analysis of a small shell-and-tube heat exchanger," Energy Conversion and Management, vol. 51, no. 5, pp. 1004–1014, 2010.
- [10] P. Bichkar, O. Dandgaval, P. Dalvi, R. Godase, and T. Dey, "Study of Shell and Tube Heat Exchanger with the Effect of Types of Baffles," Procedia Manufacturing, vol. 20, pp. 195–200, 2018. [Online]. Available: https://doi.org/10.1016/j.promfg.2018.02.028
- [11] Q. Wang, G. Chen, Q. Chen, and M. Zeng, "Review of Improvements on shell-and-tube heat exchangers with helical baffles," Heat Transfer Engineering, vol. 31, no. 10, pp. 836–853, 2010.
 - [12] N. Mukilarasan, R. Karthikeyan, S. Ramalingam, D. Dillikannan, J. Ravikumar, S. Sampath, and G. Kaliyaperumal, "Influence of baffles in heat transfer fluid characteristics using CFD evaluation," International Journal of Ambient Energy, vol. 43, no. 1, pp. 7088–7100, 2022. [Online]. Available: https://doi.org/10.1080/01430750.2022.2063175
- [13] A. El Maakoul, A. Laknizi, S. Saadeddine, M. El Metoui, A. Zaite, M. Meziane, and A. Ben Abdellah, "Numerical comparison of shell-side performance for shell and tube heat exchangers with trefoil-hole, helical and segmental baffles," Applied Thermal Engineering, vol. 109, pp. 175–185, 2016. [Online]. Available: http://dx.doi.org/10.1016/j.applthermaleng.2016.08.067
- [14] H. R. Abbasi, E. Sharifi Sedeh, H. Pourrahmani, and M. H. Mohammadi, "Shape optimization of segmental porous baffles for enhanced thermo-hydraulic performance of shell-and-tube heat exchanger," Applied Thermal Engineering, vol. 180, no. July, 2020.
- [15] X. Zhang, D. Han, W. He, C. Yue, and W. Pu, "Numerical simulation on a novel shell-and-tube heat exchanger with screw cinquefoil orifice baffles," vol. 9, no. 8, pp. 1–12, 2017. [Online]. Available: https://doi.org/10.1177/1687814017717665
- [16] K. Mohammadi, "Investigation of the Effects of Baffle Orientation, Baffle Cut and Fluid Viscosity on Shell Side Pressure Drop and Heat Transfer Coefficient in an E-Type Shell and Tube Heat Exchanger", doi: https://doi.org/354607677.
- [17] A. S. Alhulaifi, "Computational Fluid Dynamics Heat Transfer Analysis of Double Pipe Heat Exchanger and Flow Characteristics Using Nanofluid TiO2 with Water," Designs, vol. 8, no. 3, 2024.

- [18] M. Marcinkowski, D. Taler, J. Taler, and K. We, glarz, "Thermal calculations of four-row plate-fin and tube heat exchanger taking into account different air-side correlations on individual rows of tubes for low reynold numbers," Energies, vol. 14, no. 21, 2021.
- [19] M. Marcinkowski, D. Taler, K. We, glarz, and J. Taler, "Advancements in analyzing air-side heat transfer coefficient on the individual tube rows in finned heat exchangers: Comparative study of three CFD methods," Energy, vol. 307, no. August, p. 132754, 2024. [Online]. Available: https://doi.org/10.1016/j.energy.2024.132754
- [20] S. M. Shahril, G. A. Quadir, N. A. M. Amin, and I. A. Badruddin, "Thermo hydraulic performance analysis of a shell-and-double concentric tube heat exchanger using CFD," *International Journal of Heat and Mass Transfer*, vol. 105, pp. 781–798, Feb. 2017, doi: 10.1016/j.ijheatmasstransfer.2016.10.021.
- [21] M. A. Jamil, T. S. Goraya, M. W. Shahzad, and S. M. Zubair, "Exergoeconomic optimization of a shell-andtube heat exchanger," Energy Conversion and Management, vol. 226, p. 113462, dec 2020. [Online]. Available: https://linkinghub.elsevier.com/retrieve/pii/S019689042030995X
- [22] M. A. Alperen, E. Kayabaşi, and H. Kurt, "Detailed comparison of the methods used in the heat transfer coefficient and pressure loss calculation of shell side of shell and tube heat exchangers with the experimental results," *Energy Sources, Part A: Recovery, Utilization, and Environmental Effects*, vol. 45, no. 2, pp. 5661–5680, Jun. 2023, doi: 10.1080/15567036.2019.1672835.
- [23] P. A. D. Cruz, E. J. E. Yamat, J. P. E. Nuqui, and A. N. Soriano, "Computational Fluid Dynamics (CFD) analysis of the heat transfer and fluid flow of copper (II) oxide-water nanofluid in a shell and tube heat exchanger," Digital Chemical Engineering, vol. 3, no. September 2021, p. 100014, 2022. [Online]. Available: https://doi.org/10.1016/j.dche.2022.100014
- [24] A. Hazra, "Using the confidence interval confidently," Journal of Thoracic Disease, vol. 9, no. 10, pp. 4124–4129, oct 2017. [Online]. Available: http://jtd.amegroups.com/article/view/16406/13455 [31] J. Sauro and J. R. Lewis, How Precise Are Our Estimates? Confidence Intervals. Jeff Sauro and James R. Lewis, 2012. [Online]. Available: http://dx.doi.org/10.1016/B978-0-12-384968-7.00003-5
- [25] J. Sauro and J. R. Lewis, How Precise Are Our Estimates? Confidence Intervals. Jeff Sauro and James R. Lewis, 2012. [Online]. Available: http://dx.doi.org/10.1016/B978-0-12-384968-7.00003-5